Carbohydrate Polymers 87 (2012) 757–763

Contents lists available at SciVerse ScienceDirect

Carbohydrate Polymers

journal homepage: www.elsevier.com/locate/carbpol

Preparation of konjac glucomannan-based superabsorbent polymers by frontal polymerization

Jing Li[a], Jie Ji[a], Jun Xia[b], Bin Li[a,*]

[a] College of Food Science and Technology, Huazhong Agricultural University, Wuhan, Hubei 430070, China
[b] Yichang Institute of Products Quality Supervision and Inspecting, Yichang, Hubei 443000, China

ARTICLE INFO

Article history:
Received 30 June 2011
Received in revised form 5 August 2011
Accepted 19 August 2011
Available online 26 August 2011

Keywords:
Frontal polymerization
Konjac glucomannan
Superabsorbent polymers
Water absorbency

ABSTRACT

Frontal polymerization was used to prepare two kinds of superabsorbent polymers (SAP) called konjac glucomannan–acrylic acid–acrylamide (KGM–AA–AM) polymers and konjac glucomannan–acrylic acid–kaolin (KGM–AA–Kaolin) polymers. As preparation of KGM–AA–AM, it was found that features of front propagation including front velocity and maximum temperature (T_{max}) were dependent on the amount of acrylamide, initiator (potassium persulfate) and water, which influenced characterization of final products in the former. However, in the other polymer system, when Kaolin/AA ratio reached 0.30, the highest water absorbency was obtained, 1941 g/g in distilled water and 93 g/g in physiological saline. That indicates kaolin is a potential material to enhance water absorbency of FP products.

© 2011 Elsevier Ltd. All rights reserved.

1. Introduction

Konjac glucomannan (KGM), a water-soluble high-molecular weight heteropolysaccharide, is composed of 1,4-linked β-D-mannose and β-D-glucose units in a molar ratio of 1.6:1 with a low degree of acetyl groups at the side chain C-6 position and a molecular weight of 0.67–1.9 million on average (Maeda, Shimahara, & Sugiyamsa, 1980; Shimahara, Suzuki, Sugiyama, & Nishizawa, 1975). It has been generally used in food, medical and chemical engineering, and other fields because of its unique physical and chemical properties. In our previous work (Li et al., 2009), we prepared KGM-graft-acrylic acid hydrogel by frontal polymerization (FP) and found it display high water absorption rate. These results make us carry out further research about KGM-based superabsorbent polymers.

FP is a process of converting the monomer into polymer by means of a spatially localized reaction zone which propagates through the heat release by the reaction itself (Chechilo, Khvilivitskii, & Enikolopyan, 1972). Once the reaction started, conversion of monomers to polymers needs no additional energy if the heat release is sufficiently higher than heat loss.

FP was first discovered by Chechilo and Enikolopyan in 1972. Subsequently, Chechilo and his co-workers carried out some more research works about it (Chechilo & Enikolopyan, 1974, 1975, 1976). Pojman and his co-workers demonstrated the feasibility of FP at ambient pressure later, which brought about widespread research of FP in the recent two decades.

The researches were interested in the dependence of the frontal polymerization behavior on the monomer and initiator concentration for many systems (Masere, Stewart, Meehan, & Pojman, 1999; Masere et al., 2000; Pojman, Willis, Fortenberry, Ilyashenko, & Khan, 1995). In addition, McFarland, Popwell, and Pojman (2004, 2006) successfully produced microcapsules containing initiator to obtain a longer pot life in FP.

Acrylamide was commonly used as a monomer. Fortenberry and Pojman prepared polyacrylamide with potassium persulfate as initiator via frontal polymerization. In the quest to synthesize polyacrylamide intermolecular imidization occurred at the high temperatures in the front, resulting in a crosslinked polymer (Fortenberry & Pojman, 2000). Pujari et al. triggered frontal polymerization of acrylamide by the simple addition of a minute, specific volume of water. They investigated effect of type and concentration of redox couple and volume of water on front velocity, front temperature, shape of front and yield (Pujari, Inamdar, Ponrathnam, & Kulkarni, 2007). Chen, Hu, Yu, Chen, and Pojman (2007) reported the first synthesis of poly (*N*-methylolacrylamide) (PNMA) via free-radical frontal polymerization with solid monomers at ambient pressure and claimed that solvent-free FP could be exploited as a means for preparation of PNMA with the potential advantage of higher throughput than solvent-based methods.

The frontal photopolymerization was one of FP that exposes monomer continuously to UV radiation in the presence of a photobleachable initiator (Crivello, 2005, 2007; Crivello & Bulut, 2005;

* Corresponding author. Tel.: +86 027 63730040; fax: +86 027 87282966.
E-mail address: libinfood@mail.hzau.edu.cn (B. Li).

0144-8617/$ – see front matter © 2011 Elsevier Ltd. All rights reserved.
doi:10.1016/j.carbpol.2011.08.060

Crivello, Falk, & Zonca, 2004; Cui, Yang, Zeng, Zeng, & Chen, 2007a, 2007b; Ivanov & Decker, 2004). Frontal polymerization with Thiol-Ene Systems were thoroughly studied by Devadoss, Pojman, and Volpert (2006) and Pojman, Varisli, Perryman, Edwards, and Hoyle (2004).

Mariani, Alzari, Monticelli, Pojman, and Caria (2007, 2008) prepared epoxy polymeric nanocomposites which showed characteristics similar or even better than those prepared by the conventional polymerization. Then, they studied frontal curing of a triepoxy resin using two different BF3-amine initiators in the presence of various amounts of two fillers (Scognamillo, Bounds, Luger, Mariani, & Pojman, 2010). Chen et al. synthesized epoxy resin–polyurethane hybrid networks (Chen, Tian, Chen, & Hu, 2006), segmented polyurethane (Chen, Sui, & Chen, 2005), polyurethane–nanosilica hybrids (Chen, Sui, Chen, & Pojman, 2005), urethane–acrylate copolymers (Hu, Chen, Tian, Pojman, & Chen, 2006), poly(*N*-vinyl pyrrolidone) (Cai, Chen, & Chen, 2008), poly(*N*-methylolacrylamide) (Chen et al., 2007), and poly(*N*-methylolacrylamide) hybrids (Fang, Chen, & Chen, 2009; Hu, Fang, Yu, Chen, & Chen, 2007), poly(2-hydroxyethyl acrylate-co-vinyl versatate) amphiphilic gels (Tu, Chen, Fang, Wang, & Chen, 2010) and fluorescent quantum dot-polymer nanocomposites (Fang, Chen, Wang, & Chen, 2010) by FP.

Chekanov and Pojman (2000) used FP to prepare functionally gradient materials. Feng, Li, Yan, Zhu, and Ge (2010) carried out PNIPAm hydrogels by FP used as drug delivery devices. The production of optical gradient materials via frontal polymerization was repeatedly mentioned in recent years (Evstratova, Antrim, Fillingane, & Pojman, 2006; Lewis, Debisschop, Pojman, & Volpert, 2005; Masere, Lewis, & Pojman, 2001).

Yan, Zhang, Lu, Su, and Ge (2005) produced super-absorbent polymers (SAP) based on acrylic acid grafted onto starch via FP. After that, some further studies on starch or CMC grafting poly (acrylic acid) hydrogels were carried out by Yan's group (Lu, Yan, & Ge, 2007; Yan, Zhang, Lu, Su, & Ge, 2006; Yan, Lu, Zhang, Ma, & Ge, 2007). Recently, Mariani et al. who dedicated many papers on this topic (Fiori, Malucelli, Mariani, Ricco, & Casazza, 2002; Fiori, Mariani, Ricco, & Russo, 2003; Mariani, Bidali, Fiori, Malucelli, & Sanna, 2003; Mariani, Fiori, Bidali, Alzari, & Malucelli, 2008; Mariani, Nuvoli, Alzari, & Pini, 2008) prepared super water absorbent hydrogels obtained from acrylamide and 3-sulfopropyl acrylate, potassium salt in the presence of *N*,*N*-methylenebisacrylamide as a crosslinker by FP (Scognamillo, Alzari, Nuvoli, & Mariani, 2010).

In our previous work (Li et al., 2009), we focused on studying the influence of the relative reaction components on the front parameters and polymer properties through frontal polymerization synthesis of konjac glucomannan-graft-acrylic acid polymers. In this study, KGM–acrylic acid–acrylamide polymers and KGM–acrylic acid–kaolin polymers were synthesized by frontal polymerization and effects of different conditions on the front propagation and products characterization were investigated. Inorganic compound (kaolin) was used to lower the cost and enhance the properties of superabsorbent polymers.

2. Materials and methods

2.1. Materials

Konjac glucomannan (KGM) was purchased from Shiyan Huaxianzi Konjac Productions Co., Ltd. Acrylic acid (AA) was purchased from Tianjing Guangfu Fine Chemical Research Institute; methylene bisacrylamide (MBA) and kaolin were purchased from Tianjin BoDi Chemical Company; acrylamide (AM), sodium hydroxide and potassium persulfate (KPS) were purchased from Sinopharm Chemical Reagent Company. They were all of A.R. grade and used without further purification.

2.2. Preparation of reactant mixture

KGM was purified as our previous work (Li & Xie, 2004) and distilled water were mixed and stirred magnetically at 30 °C for 1 h to ensure the fully swelling of KGM. Acrylic acid was partially neutralized with solution of sodium hydroxide in distilled water at ice bath. Then potassium persulfate and methylene bisacrylamide were dissolved in distilled water respectively. Solution of acrylamide and kaolin suspension were prepared. Then solutions of the partially neutralized acrylic acid, initiator (potassium persulfate), crosslinking agent (methylene bisacrylamide) and acrylamide were added to the solution of KGM (which named KGM–AA–AM system). In the other system (KGM–AA–Kaolin), kaolin suspension replaced solution of acrylamide. The mixture was stirred magnetically at 30 °C for 20 min. In this experiment, amounts of KGM, AA and MBA were constant.

2.3. Frontal polymerization

The prepared mixture was poured into a 180 mm (D = 15 mm) long test tube which was clamped to an iron support in a drying oven. Frontal polymerization was initiated by putting a hot soldering iron on the top of the tube until the formation of the traveling front became evident. After the reaction was end, the tube was removed from iron support and cooled to room temperature. The reaction product was cut into small pieces (1–3 mm) which were immersed in a solution (70 vol%) of aqueous ethanol for 24 h to remove water-soluble materials and unreacted monomer. Then the pieces were dehydrated with ethanol and dried in a vacuum oven at 70 °C until the weight of the specimen was constant.

2.4. Frontal velocity and temperature measurements

The frontal velocities were determined by measuring the distance that the front traveled as a function of time which was in terms of centimeters per minute (cm/min). The temperature change was recorded by a K-type thermocouple which was immersed at a 6 cm distance from the free surface.

2.5. Water absorbency measurement

The measurement of the absorbency of SAP was conducted at room temperature by a filtration method, and distilled water or physiological saline was used as the liquids to be absorbed. The samples were immersed in distilled water or physiological saline for a period of time. The swollen samples were filtered through a 100 mesh filtration fabric for 10 min. The weight of dry SAP was marked as W_o. The weight of the wet filtration fabric was measured and marked as W_f. The weight of the filtration fabric including the swollen sample was measured and marked as W_s. The absorption rate of SAP was calculated as:

$$\text{Absorption rate } Q = \frac{W_s - W_o - W_f}{W_o}$$

2.6. Characterization

2.6.1. IR

The powdered SAP were blended with potassium bromide and laminated, and the IR of the films were recorded at room temperature using a Nicolet (USA) Nexus 470 FTIR spectrometer at a resolution of 4 cm^{-1} in the range of 400–4000 cm^{-1}.

2.6.2. SEM

The microstructure of a dry SAP sample was investigated by means of a scanning electron microscope (SEM, JSM-6390/LV). The dry sample was ground into powder, mounted on a metal stub, and coated with gold. Subsequently, its microstructure was observed by the SEM.

2.6.3. DSC

The dry SAP sample (5 mg) was placed in aluminum pan. The differential scanning calorimetry of the mixture performed under a nitrogen atmosphere with a flow capacity of 20 ml/min by a DSC 204-F1 (NETZSCH, Germany) from 30 to 450 °C at a heating rate of 10 K/min.

3. Results and discussion

3.1. KGM–AA–AM polymers

Because of the difference in refractive index between the unreacted monomer mixture and the synthesized polymer, the propagation of the front can be optically monitored and recorded its position as a function of time. The frontal propagated at a constant velocity even with a lot of bubbles resulted from the evaporation of water. The reaction of polymerization and crosslinking was triggered when the front arrived. A large amount of heat was released that caused rapid increasing of temperature over a short distance. The reacted heat sustained the propagation of front. The rapid temperature increasing may result in some special properties of the FP products.

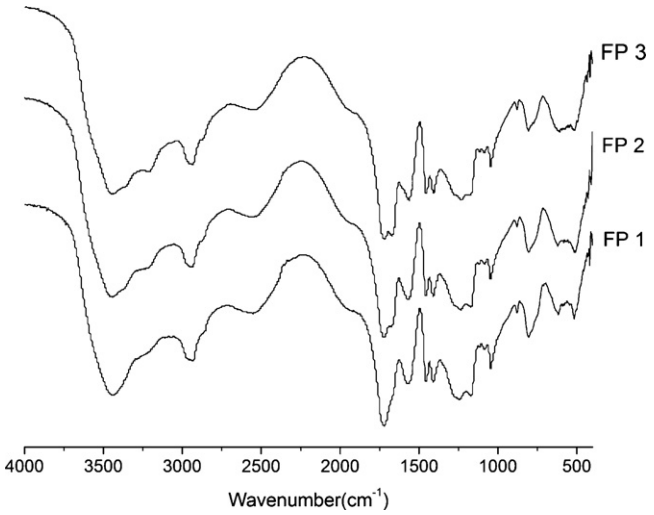

Fig. 1. FT-IR spectra of KGM–AA–AM polymers.

Front velocity and its maximum temperature are the parameters of main interest. Table 1 shows the effect of different amounts of acrylamide on the front propagation. Acrylamide was a monomer in reaction and three levels of its amount were investigated. Front velocity increased with increasing the amount of acrylamide, from 0.45 to 0.99 cm/min, because acrylamide has a high reactivity. And the increase of acrylamide amount caused an increase of T_{max} from 101 to 115 °C.

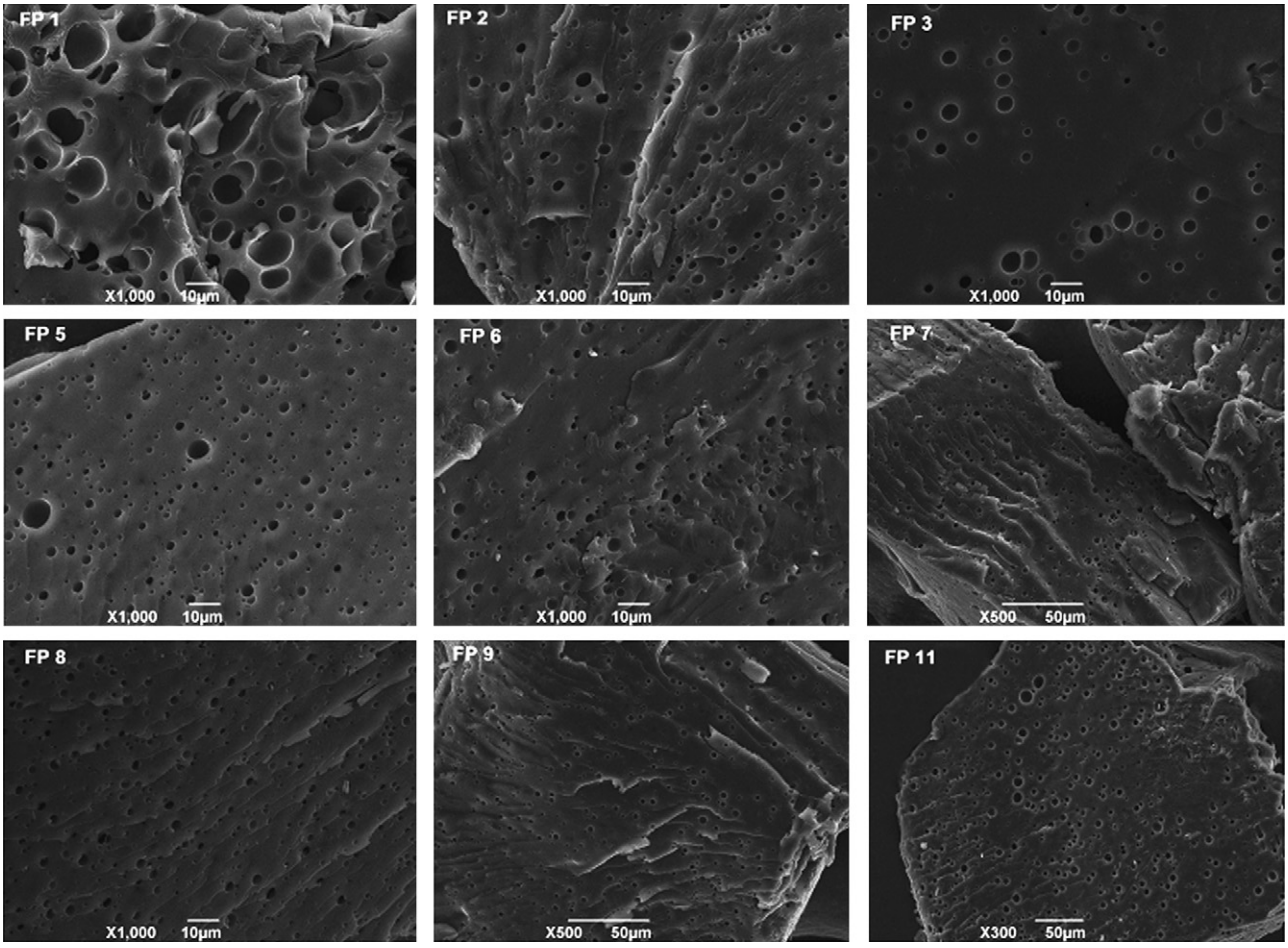

Fig. 2. SEM images of KGM–AA–AM polymers.

Table 1
Effects of different conditions to the front propagation and liquid absorbency.

No.[a]	AM/AA (wt/wt)	KPS/AA (wt/wt)	Water/AA (wt/wt)	Velocity (cm/min)[b]	T_{max} (°C)[b]	Water absorbency in d-water (g/g) ± SD[b]	Water absorbency in physiological saline (g/g) ± SD[b]
FP1	0.10	0.015	2.0	0.45 ± 0.02	101 ± 1	717 ± 37	59 ± 2
FP2	0.25	0.015	2.0	0.73 ± 0.01	106 ± 1	359 ± 19	49 ± 2
FP3	0.40	0.015	2.0	0.99 ± 0.02	115 ± 2	276 ± 9	44 ± 2
FP4	0.25	0.015	2.0	0.73 ± 0.01	106 ± 1	359 ± 19	49 ± 2
FP5	0.25	0.025	2.0	0.78 ± 0.01	112 ± 2	277 ± 16	48 ± 2
FP6	0.25	0.035	2.0	0.84 ± 0.04	115 ± 1	240 ± 11	45 ± 1
FP7	0.25	0.045	2.0	0.91 ± 0.03	116 ± 2	204 ± 9	43 ± 1
FP8	0.25	0.055	2.0	0.95 ± 0.01	117 ± 3	164 ± 12	41 ± 1
FP9	0.25	0.015	1.8	0.99 ± 0.01	123 ± 3	239 ± 13	42 ± 1
FP10	0.25	0.015	2.0	0.73 ± 0.01	106 ± 1	359 ± 19	49 ± 2
FP11	0.25	0.015	2.2	0.56 ± 0.01	103 ± 2	630 ± 21	56 ± 4

[a] FP2, FP4, and FP10 were the same experiment.
[b] Mean ± standard deviation, SD; $n = 3$.

Five levels were selected to investigate the effect of initiator (potassium persulfate) on FP, from 0.015 to 0.055 (ratio of initiator/AA). Results were shown in Table 1. Front velocity increased from 0.73 to 0.95 cm/min, with increasing the amount of initiator, for the increasing initiator amount enhancing the radical concentration. Besides, the dependence of the front velocity on the initiator amount fitted a power function, with the power 0.21. This result was supported by previous reports (Davtyan, Zhirkov, & VolPfson, 1984; Li et al., 2009; Pojman et al., 1995). The increase of initiator amount caused an increase of T_{max} from 106 to 117 °C. The experiments were all performed under nonadiabatic conditions and the higher velocity could reduce heat loss. For this reason, the dependence of T_{max} on initiator was similar as front velocity.

Effect of different amounts of water on FP was shown in Table 1. Both front velocity and T_{max} decreased with increasing amounts of water. Water was used as solvent in experiment. However, water could also be used as diluent for vapourization of water taking away some heat.

3.1.1. FT-IR spectroscopy

Fig. 1 shows the IR spectra of polymers contained with different amounts of acrylamide, in the wavenumber range of 4000–400 cm^{-1}. The absorption band at 3440 cm^{-1} was assigned to the stretching of N–H and O–H of polymer and absorption band at 2935 cm^{-1} was assigned to the C–H of methyl groups. The characteristic absorption bands of $–COO^-$ appeared at 1718 and 1560 cm^{-1}. With the increase of AM amount, absorption bands appeared at 1674 cm^{-1} which was characteristic of $–CO–NH_2$.

3.1.2. SEM images and water absorbency of KGM–AA–AM polymers

SEM images (Fig. 2) showed KGM–AA–AM polymers have porous structure, but their pore diameter and density decreased compared to KGM–AA polymers (Li et al., 2009). It could be attributed to the increase of crosslinking density of polymers as the addition of AM. Another reason might be evaporation of water was insufficient because of fast front velocity.

From Table 1 it can be seen that when AM/AA ratio increased from 0.10 to 0.40, the water absorption rate in distilled water and physiological saline decreased from 717 to 276 g/g and 59 to 44 g/g, respectively. Water absorption rate in distilled water decreased from 359 to 164 g/g as the initiator/AA ratio raised from 0.015 to 0.055 and in physiological saline the rate decreased from 49 to 41 g/g. While the amount of water increased, both water absorption rate in distilled water and physiological saline increased. SAP in our experiment were lightly crosslinked hydrophilic polymers whose water absorbency was affected by several chemical and structural factors such as hydrophilicity of polymer backbone, degree of crosslinking, degree of ionization and amount of ionic groups and eventual presence of porosity (Lenzi et al., 2003). More AM and initiator led more reaction heat release which could increase the amount of low molecular weight polymer resulting in the decrease of water absorption rate. The effect of water on water absorbency of polymers was opposite to AM and initiator because its evaporation could absorb heat.

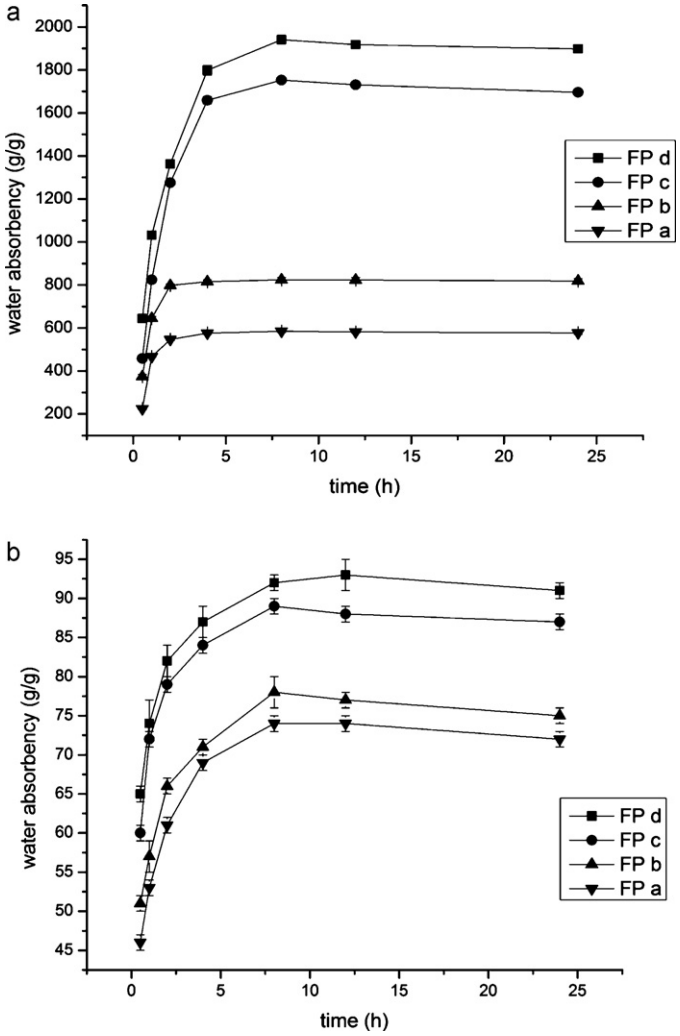

Fig. 3. Absorption kinetics of KGM–AA–Kaolin polymers in distilled water (a) and physiological saline (b).

Table 2
Effect of kaolin on T_{max} and water absorbency.

No.	Kaolin/AA (wt/wt)	Maximum temperature (°C) ± SD[a]	Water absorbency in distilled water (g/g) ± SD[a]	Water absorbency in physiological saline (g/g) ± SD[a]
FP a	0.01	106.3 ± 0.6	585 ± 6	74 ± 1
FP b	0.10	103.5 ± 0.6	824 ± 11	78 ± 2
FP c	0.20	98.0 ± 1.0	1753 ± 8	89 ± 1
FP d	0.30	94.3 ± 0.5	1941 ± 20	93 ± 2

[a] Mean ± standard deviation, SD; $n = 3$.

3.2. KGM–AA–Kaolin polymers

The reaction system presented white colour when kaolin suspension was added. It is difficult to find the boundary between unreacted monomer mixture and the synthesized polymer, thus the front could not be optically monitored. However, front velocity was unknown in this reaction while the temperature could be recorded by a K-type thermocouple. T_{max} reduced gradually as amount of kaolin increased (Table 2).

3.2.1. Water absorbency of KGM–AA–Kaolin polymers

As is shown in Table 2, water absorption rate in distilled water increased from 585 to 1941 g/g as the Kaolin/AA ratio raised from 0.01 to 0.30 and in physiological saline the rate increased from 74 to 93 g/g. These data revealed that the reaction temperature of FP does affect properties of the obtained samples. Kaolin could be taken as diluent for its absorbing heat in reaction. As a result, polymerization slowed down and less low molecular weight polymer was synthesized resulting in high water absorbency of final products. In addition, a large number of hydroxy and charge of kaolin contributed to water absorbency of KGM–AA–Kaolin polymers.

Fig. 3 represented absorption kinetics curve of KGM–AA–Kaolin polymers. Process of water absorption could be divided into three stages: quick absorption stage, saturation stage and dissolving stage. Water absorption rate of all samples reached the highest at 8 h in distilled water, then reduced slightly. The same trend displayed in physiological saline.

3.2.2. SEM images of KGM–AA–Kaolin polymers

As can be observed in Fig. 4, when Kaolin/AA ratios were 0.01 and 0.10, microstructure of polymers was similar to KGM–AA polymers (Li et al., 2009). When the ratio reached 0.20 and 0.30, lamina structure and dense pore structure appeared which raised specific surface area to enhance the water absorbency. It is supposed that these pores are the regions of water permeation and interaction sites of external stimuli with the hydrophilic groups of the graft copolymers (Pourjavadi, Ayyari, & Amini-Fazl, 2008). The dramatic enhancements in absorbing behavior could be attributed to structural improvements in the hydrogel produced by FP and introduction of kaolin.

3.2.3. FT-IR spectroscopy

Fig. 5 shows the IR spectra of polymers contained with different amounts of kaolin, in the wavenumber range of 4000–400 cm^{-1}. The absorption band at 3200–3500 cm^{-1} were assigned to the stretching of –OH, which shifted to a little higher wavenumber as the increase of kaolin amount. The absorption bands at 2945 cm^{-1} were assigned to the stretching of methyl groups. A strong band at 1720 cm^{-1} was attributed to stretching vibrational absorption of $–COO^-$. The bands appearing at 1408 cm^{-1} were attributed to the bending vibration of $–COO^-$. Stretching vibrational absorption of Si–O appeared around 1045 cm^{-1}.

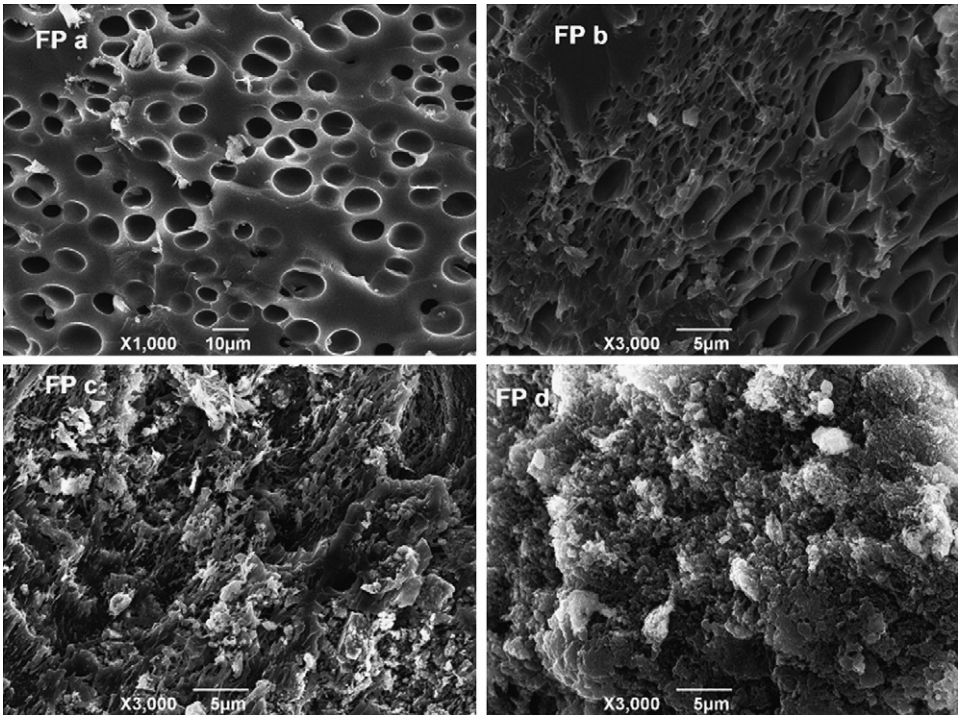

Fig. 4. SEM images of KGM–AA–Kaolin polymers.

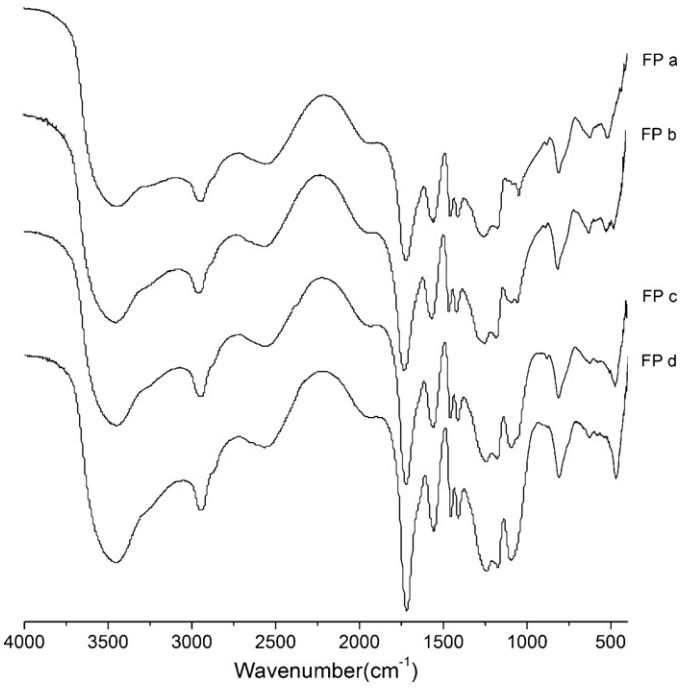

Fig. 5. FT-IR spectra of KGM–AA–Kaolin polymers.

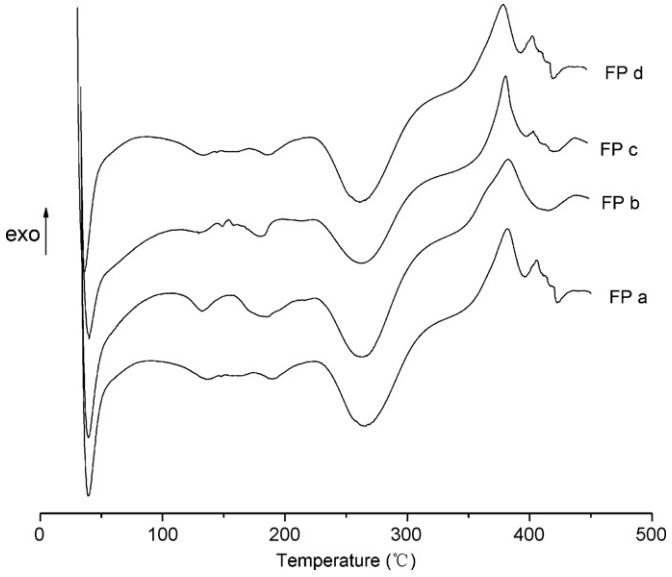

Fig. 6. DSC thermograms of KGM–AA–Kaolin polymers.

3.2.4. Thermal properties

The DSC curves of four KGM–AA–Kaolin polymers illustrated in Fig. 6. The introduction of inorganic fillers to a polymer matrix affected its thermal property. Endothermic peak appeared around 246 °C in all four samples which was attributed to melting of polymers. Exothermic peak appeared around 384 °C in FP a and FP b, which was attributed to thermal decomposition of polymers. This peak shifted to 382 °C and 369 °C in FP c and FP d respectively. The results indicated heat stability of polymers reduced with the increase of kaolin.

4. Conclusions

In this article, we reported the synthesis of KGM–acrylic acid–acrylamide polymers and KGM–acrylic acid–kaolin polymers by frontal polymerization, a novel method to produce functional materials.

The features of front propagation of KGM–AA–AM polymers including front velocity and T_{max} were influenced by the amount of acrylamide, initiator and water. T_{max} in synthesis of KGM–AA–Kaolin polymers reduced gradually as amount of kaolin increased while front velocity was hard to record by common method.

The polymers were characterized by FT-IR, SEM or DSC. Water absorbency of polymers was also investigated. It is worth mentioning that fast front velocity has negative effects on water absorbency. In particular, water absorption rate of KGM–acrylic acid–kaolin polymers in distilled water reached to 1941 g/g, which indicates kaolin is a potential material to enhance water absorbency of FP products.

The above results allow us to conclude that FP is a fast and reliable technique for polymer synthesis.

Acknowledgment

Financial support from contract grant sponsor: The National Natural Science Foundation of China (Grant No. 31071607).

References

Cai, X., Chen, S., & Chen, L. (2008). Solvent-free free-radical frontal polymerization: A new approach to quickly synthesize poly(*N*-vinylpyrrolidone). *Journal of Polymer Science Part A: Polymer Chemistry*, *46*(6), 2177–2185.

Chechilo, N., & Enikolopyan, N. (1974). Structure of the polymerization wave front and propagation mechanism of the polymerization reaction. *Doklady Physical Chemistry*, *214*, 174–176.

Chechilo, N., & Enikolopyan, N. (1975). Effect of the concentration and nature of initiations on the propagation process in polymerization. *Doklady Physical Chemistry*, *221*, 392–394.

Chechilo, N., & Enikolopyan, N. (1976). Effect of pressure initial temperature of the reaction mixture during propagation of a polymerization reaction. *Doklady Physical Chemistry*, *230*, 840–843.

Chechilo, N. M., Khvilivitskii, R. J., & Enikolopyan, N. S. (1972). On the phenomenon of polymerization reaction spreading. *Doklady Akademii Nauk*, *204*, 1180–1181.

Chekanov, Y. A., & Pojman, J. A. (2000). Preparation of functionally gradient materials via frontal polymerization. *Journal of Applied Polymer Science*, *78*(13), 2398–2404.

Chen, S., Sui, J. J., & Chen, L. (2005). Segmented polyurethane synthesized by frontal polymerization. *Colloid and Polymer Science*, *283*(8), 932–936.

Chen, S., Sui, J. J., Chen, L., & Pojman, J. A. (2005). Polyurethane–nanosilica hybrid nanocomposites synthesized by frontal polymerization. *Journal of Polymer Science Part A: Polymer Chemistry*, *43*(8), 1670–1680.

Chen, S., Tian, Y., Chen, L., & Hu, T. (2006). Epoxy resin/polyurethane hybrid networks synthesized by frontal polymerization. *Chemistry of Materials*, *18*(8), 2159–2163.

Chen, L., Hu, T., Yu, H., Chen, S., & Pojman, J. A. (2007). First solvent-free synthesis of poly(*N*-methylolacrylamide) via frontal free-radical polymerization. *Journal of Polymer Science Part A: Polymer Chemistry*, *45*(18), 4322–4330.

Crivello, J. V. (2005). Investigation of the photoactivated frontal polymerization of oxetanes using optical pyrometry. *Polymer*, *46*(26), 12109–12117.

Crivello, J. V. (2007). Hybrid free radical/cationic frontal photopolymerizations. *Journal of Polymer Science Part A: Polymer Chemistry*, *45*(18), 4331–4340.

Crivello, J. V., & Bulut, U. (2005). Photoactivated cationic ring-opening frontal polymerizations of oxetanes. *Designed Monomers and Polymers*, *8*(6), 517–531.

Crivello, J. V., Falk, R., & Zonca, M. R. (2004). Photoinduced cationic ring-opening frontal polymerizations of oxetanes and oxiranes. *Journal of Polymer Science Part A: Polymer Chemistry*, *42*(7), 1630–1646.

Cui, Y. Y., Yang, J. W., Zeng, Z. H., Zeng, Z., & Chen, Y. L. (2007a). Monitoring frontal photopolymerization by electroresistance. *European Polymer Journal*, *43*(9), 3912–3922.

Cui, Y. Y., Yang, J. W., Zeng, Z. H., Zeng, Z., & Chen, Y. L. (2007b). Unique morphology and properties study of polyacrylate obtained via frontal photopolymerization. *Polymer*, *48*(20), 5994–6001.

Davtyan, S. P., Zhirkov, P. V., & VolPfson, S. A. (1984). Problems of non-isothermal character in polymerisation processes. *Russian Chemical Reviews*, *53*, 150–163.

Devadoss, D. E., Pojman, J. A., & Volpert, V. A. (2006). Mathematical modeling of thiol-ene frontal polymerization. *Chemical Engineering Science*, *61*(4), 1261–1275.

Evstratova, S. I., Antrim, D., Fillingane, C., & Pojman, J. A. (2006). Isothermal frontal polymerization: Confirmation of the isothermal nature of the process and the effect of oxygen and polymer seed molecular weight on front propagation. *Journal of Polymer Science Part A: Polymer Chemistry*, *44*(11), 3601–3608.

Fang, Y., Chen, L., & Chen, S. (2009). Facile and quick synthesis of poly(*N*-methylolacrylamide)/polyhedral oligomeric silsesquioxane (POSS) graft copolymer hybrids via frontal polymerization. *Journal of Polymer Science Part A: Polymer Chemistry*, *47*(4), 1136–1147.

Fang, Y., Chen, L., Wang, C. F., & Chen, S. (2010). Facile synthesis of fluorescent quantum dot-polymer nanocomposites via frontal polymerization. *Journal of Polymer Science Part A: Polymer Chemistry*, *48*(10), 2170–2177.

Feng, Q., Li, F., Yan, Q. Z., Zhu, Y. C., & Ge, C. C. (2010). Frontal polymerization synthesis and drug delivery behavior of thermo-responsive poly(*N*-isopropylacrylamide) hydrogel. *Colloid and Polymer Science*, *288*(8), 915–921.

Fiori, S., Malucelli, G., Mariani, M., Ricco, L., & Casazza, E. (2002). Interpenetrating polydicyclopentadiene/polyacrylate networks obtained by simultaneous non-interfering frontal polymerization. *e-Polymers*, *57*, 1–10.

Fiori, S., Mariani, A., Ricco, L., & Russo, S. (2003). First synthesis of a polyurethane by frontal polymerization. *Macromolecule*, *36*(8), 2674–2679.

Fortenberry, D. I., & Pojman, J. A. (2000). Solvent-free synthesis of polyacrylamide by frontal polymerization. *Journal of Polymer Science Part A: Polymer Chemistry*, *38*(7), 1129–1135.

Hu, T., Chen, S., Tian, Y., Pojman, J. A., & Chen, L. (2006). Frontal free-radical copolymerization of urethane–acrylates. *Journal of Polymer Science Part A: Polymer Chemistry*, *44*(9), 3018–3024.

Hu, T., Fang, Y., Yu, H., Chen, L., & Chen, S. (2007). Synthesis of poly(*N*-methylolacrylamide)/polymethylacrylamide hybrids via frontal free-radical polymerization. *Colloid and Polymer Science*, *285*(8), 891–898.

Ivanov, V. V., & Decker, C. (2004). Kinetic study of photoinitiated frontal polymerization. *Polymer International*, *50*(1), 113–118.

Lenzi, F., Sannino, A., Borriello, A., Porro, F., Capitani, D., & Mensitieri, G. (2003). Probing the degree of crosslinking of a cellulose based superabsorbing hydrogel through traditional and NMR techniques. *Polymer*, *44*(5), 1577–1588.

Lewis, L. L., Debisschop, C. S., Pojman, J. A., & Volpert, V. A. (2005). Isothermal frontal polymerization: Confirmation of the mechanism and determination of factors affecting the front velocity, front shape, and propagation distance with comparison to mathematical modeling. *Journal of Polymer Science Part A: Polymer Chemistry*, *43*(23), 5774–5786.

Li, B., & Xie, B. J. (2004). Synthesis and characterization of konjac glucomannan/poly(vinyl alcohol) interpenetrating polymer networks. *Journal of Applied Polymer Science*, *93*, 2775–2780.

Li, J., Zhang, X., Chen, J., Xia, J., Ma, M. H., & Li, B. (2009). Frontal polymerization synthesis and characterization of konjac glucomannan-graft-acrylic acid polymers. *Journal of Polymer Science Part A: Polymer Chemistry*, *47*(13), 3391–3398.

Lu, G. D., Yan, Q. Z., & Ge, C. C. (2007). Preparation of porous polyacrylamide hydrogels by frontal polymerization. *Polymer International*, *56*(8), 1016–1020.

Maeda, M., Shimahara, H., & Sugiyamsa, N. (1980). Detailed determination of branched structure of konjac glucomannan. *Agricultural and Biological Chemistry*, *44*(2), 245–252.

Mariani, A., Bidali, S., Fiori, S., Malucelli, G., & Sanna, E. (2003). Synthesis and characterization of a polyurethane prepared by frontal polymerization. *e-Polymers*, *44*, 1–9.

Mariani, A., Alzari, V., Monticelli, O., Pojman, J. A., & Caria, G. (2007). Polymeric nanocomposites containing polyhedral oligomeric silsesquioxanes prepared via frontal polymerization. *Journal of Polymer Science Part A: Polymer Chemistry*, *45*(19), 4514–4521.

Mariani, A., Bidali, S., Caria, G., Monticelli, O., Russo, S., & Kenny, J. M. (2007). Synthesis and characterization of epoxy resin–montmorillonite nanocomposites obtained by frontal polymerization. *Journal of Polymer Science Part A: Polymer Chemistry*, *45*(11), 2204–2211.

Mariani, A., Fiori, S., Bidali, S., Alzari, V., & Malucelli, G. (2008). Frontal polymerization of diurethane diacrylates. *Journal of Polymer Science Part A: Polymer Chemistry*, *46*(10), 3344–3351.

Mariani, A., Nuvoli, D., Alzari, V., & Pini, M. (2008). Phosphonium-based ionic liquids as a new class of radical initiators and their use in gas-free frontal polymerization. *Macromolecules*, *41*(14), 5191–5196.

Masere, J., Stewart, F., Meehan, T., & Pojman, J. A. (1999). Period-doubling behavior in frontal polymerization of multifunctional acrylates. *CHAOS*, *9*(2), 315–322.

Masere, J., Chekanov, Y., Warren, J. R., Stewart, F. D., Al-Kaysi, R., Rasmussen, J. K., et al. (2000). Gas-free initiators for high-temperature free-radical polymerization. *Journal of Polymer Science Part A: Polymer Chemistry*, *38*(21), 3984–3990.

Masere, J., Lewis, L. L., & Pojman, J. A. (2001). Optical gradient materials produced via low-temperature isothermal frontal polymerization. *Journal of Applied Polymer Science*, *80*(4), 686–691.

McFarland, B., Popwell, S., & Pojman, J. A. (2004). Free-radical frontal polymerization with a microencapsulated initiator. *Macromolecules*, *37*(18), 6670–6672.

McFarland, B., Popwell, S., & Pojman, J. A. (2006). Free-radical frontal polymerization with a microencapsulated initiator: Characterization of microcapsules and their effect on pot life, front velocity, and mechanical properties. *Macromolecules*, *39*(1), 55–63.

Pojman, J. A., Willis, J., Fortenberry, D., Ilyashenko, V., & Khan, A. (1995). Factors affecting propagating fronts of addition polymerization: Velocity, front curvature, temperature profile, conversion, and molecular weight distribution. *Journal of Polymer Science Part A: Polymer Chemistry*, *33*(4), 643–652.

Pojman, J. A, Varisli, B., Perryman, A., Edwards, C., & Hoyle, C. (2004). Frontal polymerization with thiol-ene systems. *Macromolecules*, *37*(3), 691–693.

Pourjavadi, A., Ayyari, M., & Amini-Fazl, M. S. (2008). Taguchi optimized synthesis of collagen-g-poly(acrylic acid)/kaolin composite superabsorbent hydrogel. *European Polymer Journal*, *44*, 1209–1216.

Pujari, N. S., Inamdar, S. R., Ponrathnam, S., & Kulkarni, B. D. (2007). Water-triggered frontal polymerization. *Macromolecular Rapid Communications*, *28*(1), 109–115.

Scognamillo, S., Alzari, V., Nuvoli, D., & Mariani, A. (2010). Thermoresponsive super water absorbent hydrogels prepared by frontal polymerization. *Journal of Polymer Science Part A: Polymer Chemistry*, *48*(11), 2486–2490.

Scognamillo, S., Bounds, C., Luger, M., Mariani, A., & Pojman, J. A. (2010). Frontal cationic curing of epoxy resins. *Journal of Polymer Science Part A: Polymer Chemistry*, *48*(9), 2000–2005.

Shimahara, H., Suzuki, H., Sugiyama, N., & Nishizawa, K. (1975). Isolation and characterization of oligosaccharides from a enzymic hydrolisate of konjac glucomannan. *Agricultural and Biological Chemistry*, *39*(2), 293–299.

Tu, J., Chen, L., Fang, Y., Wang, C. F., & Chen, S. (2010). Facile synthesis of amphiphilic gels by frontal free-radical polymerization. *Journal of Polymer Science Part A: Polymer Chemistry*, *48*(4), 823–831.

Yan, Q. Z., Zhang, W. F., Lu, G. D., Su, X. T., & Ge, C. C. (2005). Frontal copolymerization synthesis and property characterization of starch-graft-poly(acrylic acid) hydrogels. *Chemistry – A European Journal*, *11*(22), 6609–6615.

Yan, Q. Z., Zhang, W. F., Lu, G. D., Su, X. T., & Ge, C. C. (2006). Frontal polymerization synthesis of starch-grafted hydrogels: Effect of temperature and tube size on propagating front and properties of hydrogels. *Chemistry – A European Journal*, *12*(12), 3303–3309.

Yan, Q. Z., Lu, G. D., Zhang, W. F., Ma, X. H., & Ge, C. C. (2007). Frontal polymerization synthesis of monolithic macroporous polymers. *Advanced Functional Materials*, *17*(16), 3355–3362.